This article was downloaded by: [University of California, San Diego]
On: 08 August 2012, At: 14:19
Publisher: Taylor & Francis
Informa Ltd Registered in England and Wales Registered Number: 1072954
Registered office: Mortimer House, 37-41 Mortimer Street, London W1T 3JH, UK

Molecular Crystals and Liquid Crystals

Publication details, including instructions for authors and subscription information:
http://www.tandfonline.com/loi/gmcl20

Light-Induced Nonlinear Rotations of Nematic Liquid Crystal Droplets Trapped in Laser Tweezers

Etienne Brasselet* [a], Tadas Bal[cbreve]iūnas [b], Naoki Murazawa [b], Saulius Juodkazis [b] & Hiroaki Misawa [b]

[a] Laboratoire CPMOH Université, Talence Cedex, France

[b] Research Institute for Electronic Science, Hokkaido University, Sapporo, Japan

Version of record first published: 05 Oct 2009

To cite this article: Etienne Brasselet*, Tadas Bal[cbreve]iūnas, Naoki Murazawa, Saulius Juodkazis & Hiroaki Misawa (2009): Light-Induced Nonlinear Rotations of Nematic Liquid Crystal Droplets Trapped in Laser Tweezers, Molecular Crystals and Liquid Crystals, 512:1, 143/[1989]-151/[1997]

To link to this article: http://dx.doi.org/10.1080/15421400903050780

PLEASE SCROLL DOWN FOR ARTICLE

Full terms and conditions of use: http://www.tandfonline.com/page/terms-and-conditions

This article may be used for research, teaching, and private study purposes. Any substantial or systematic reproduction, redistribution, reselling, loan,

sub-licensing, systematic supply, or distribution in any form to anyone is expressly forbidden.

The publisher does not give any warranty express or implied or make any representation that the contents will be complete or accurate or up to date. The accuracy of any instructions, formulae, and drug doses should be independently verified with primary sources. The publisher shall not be liable for any loss, actions, claims, proceedings, demand, or costs or damages whatsoever or howsoever caused arising directly or indirectly in connection with or arising out of the use of this material.

Downloaded by [University of California, San Diego] at 14:19 08 August 2012

Mol. Cryst. Liq. Cryst., Vol. 512, pp. 143/[1989]–151/[1997], 2009
Copyright © Taylor & Francis Group, LLC
ISSN: 1542-1406 print/1563-5287 online
DOI: 10.1080/15421400903050780

Downloaded by [University of California, San Diego] at 14:19 08 August 2012

Light-Induced Nonlinear Rotations of Nematic Liquid Crystal Droplets Trapped in Laser Tweezers

Etienne Brasselet[1,*], Tadas Balčiūnas[2], Naoki Murazawa[2], Saulius Juodkazis[2], and Hiroaki Misawa[2]
[1]Laboratoire CPMOH Université, Talence Cedex, France
[2]Research Institute for Electronic Science, Hokkaido University, Sapporo, Japan

We report on optically induced rotations of nematic liquid crystal droplets. We show experimentally that bipolar nematic liquid crystal droplets trapped in laser tweezers having circular polarization can exhibit nonlinear rotational motion, unlike optically trapped solid birefringent micro-plates. Such nonlinear rotations are retrieved by analyzing the polarization dynamics analysis of the light beam after it has passed through the droplet. The occurrence of complex dynamics is only found for large enough trapping power and droplet diameter. The analogy with optically induced nonlinear rotations in nematic liquid crystal films is briefly discussed.

Keywords: laser tweezers; liquid crystal droplets; optical reordering; spin angular momentum transfer

I. INTRODUCTION

Optical trapping and subsequent manipulation of matter have found many applications since the pionneering work of Ashkin almost four decades ago [1]. Indeed laser tweezers are used in the determination of optical and mechanical properties of micro/nanoparticles and materials as well as for their tracking, sorting, deposition or structural

*Also at Altechna Co. Ltd., 3 Laser Research Center, Vilnius University, Saulėtekio 10, LT-10223 Vilnius, Lithuania.

This work was carried out in the frame of a Grant-in-Aid from the Ministry of Education, Science, Sports, and Culture of Japan No.19360322.

Address correspondence to Etienne Brasselet, Laboratoire CPMOH Université Bordeaux 1, CNRS, 351 Cours de la Libération, 33405 Talence Cedex, France. E-mail: e.brasselet@cpmoh.u-bordeaux1.fr

control as summarized in recent review articles [2–5]. Liquid crystal (LC) materials are particularly well suited for optical manipulation due to their high refractive index, high birefringence, and the easy handling of spatially confined micro-systems such as droplets. Among the various existing liquid crystals ordered phases, the optical trapping, displacement and angular manipulation of nematic [6], smectic [7], and cholesteric [8] droplets have been demonstrated. Liquid crystal defects and structures are other classes of confined LC objects that can be directly manipulated using laser tweezers. This has been achieved in nematic [9], smectic [10], and cholesteric [11,12] LCs.

It is well-known that the polarization state of the trapping light beam is an essential ingredient for optical manipulation of LCs, which are birefringent materials. Indeed, similarly to earlier demonstration using birefringent calcite particles [13], LC birefringent droplets can be continuously rotated by light as a result of optical spin angular momentum deposition [6]. However there are many possible mechanisms leading to rigid body rotation of a LC droplet using light such as above-mentioned waveplate behavior, light scattering, or photon absorption processes [14]. Less understood is the role played by optical reordering inside LC droplets due to the large optical orientational nonlinearities of liquid crystals [15], which are easily accessible to standard optical trapping experiments using CW lasers. Such optical nonlinear effects have been reported both in LC droplets [16] and structures [12] in high trapping power regimes. There, the strong coupling between light and the orientational order of LCs enriches much the light-matter interaction as compared to the case of solid birefringent micro-plates where only regular rotational regimes have been reported so far.

Recently, the laser generated dynamics of radial nematic liquid crystal (NLC) droplets has been studied [17], and light-induced left/right and radial symmetry breaking were demonstrated for linear, elliptical, or circularly polarized tweezers. It follows that the role played by the polarization definitely requires a specific attention once optical reordering takes place. In addition, non-trivial nonlinear rotational behavior was observed in large pitch cholesteric droplets under linearly polarized tweezers [18], and intriguing photo-induced rotational effects were theoretically predicted in the presence of a small amount of dye added in a bipolar nematic droplet [19]. These few examples emphasize the application potential of the nonlinear behavior of optically trapped deformable materials for future micromanipulation applications.

In the present work we report on light-induced rotational motion of bipolar nematic liquid crystal droplets trapped in circularly polarized

Downloaded by [University of California, San Diego] at 14:19 08 August 2012

laser tweezers. We show experimentally that nonlinear rotations take place in presence of optical reordering inside the droplet. Such nonlinear regimes are retrieved by analyzing the polarization dynamics of the trapping beam at the output of the droplet. Complex dynamics is only found for large enough trapping power and droplet diameters. Finally, the analogy with previously observed complex collective molecular rotations in nematic liquid crystal films [20–22], where the optical orientational nonlinearities are known to play a crucial role, is briefly discussed.

II. EXPERIMENTAL SET-UP

Laser trapping and manipulation of liquid crystals droplets is carried out using a Nd:YAG CW laser operating at wavelength $\lambda = 1064\,\text{nm}$ and a microscope, as shown in Figure 1. The laser trap is set with high numerical aperture objective lens (NA = 1.3) whose entrance pupil is suitably fulfilled by the incoming beam by using a pair of collimation lenses (see 'collimation control' box in Fig. 1). The beam spot diameter is therefore of the order of the wavelength, namely 1 μm. The optical trapping power is adjusted using a half waveplate combined with a polarizer (see 'power control' box in Fig. 1) and is obtained from the

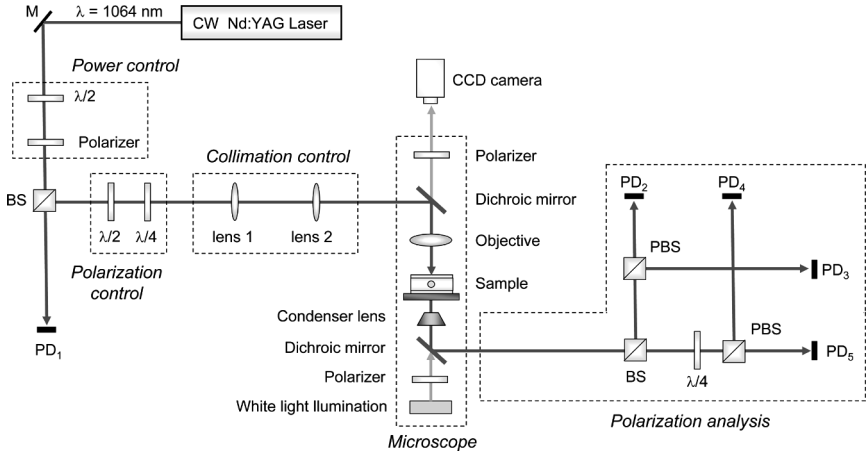

FIGURE 1 Experimental set-up. The optical trap is obtained from a CW Nd:YAG laser radiation at wavelength $\lambda = 1064\,\text{nm}$ that is focused using a microscope objective with large numerical aperture (NA = 1.3). M: mirror; $\lambda/2$: half waveplate; $\lambda/4$: quarter waveplate; BS: beamsplitter; PBS: polarizing beamsplitter; PD*i*: photodiode.

Downloaded by [University of California, San Diego] at 14:19 08 August 2012

Downloaded by [University of California, San Diego] at 14:19 08 August 2012

photodiode (PD) PD_1. The ellipticity and the position of the polarization ellipse's long axis of the incident light beam are controlled by a pair of half and quarter waveplates (see 'polarization control' box in Fig. 1). Finally, the droplets orientation dynamics is monitored (i) by imaging the droplet under white light illumination through crossed polarizers and (ii) by analyzing the polarization changes of the trapping beam after at the output of the droplet (see 'polarization analysis' box in Fig. 1). Taking z as the light propagation direction, photodiodes PD_2 and PD_3 measure respectively the power of the x- and y-polarized electric field components, from which the first reduced Stokes parameter is deduced, $s_1 = (V_2 - V_3)/(V_2 + V_3)$, where $V_{2,3}$ are the voltage values detected by $PD_{2,3}$. Similarly, photodiodes PD_4 and PD_5 respectively measure the power of the left- and right-handed circularly polarized electric field components by placing a quarter waveplate at 45° of the polarizing beam splitter main axes. The third reduced Stokes parameter is then deduced, $s_3 = (V_4 - V_5)/(V_4 + V_5)$. Before any measurement in presence of a trapped droplet, the apparatus is calibrated by using well-defined input polarization ellipse orientation and ellipticity. In addition, lenses (not shown on Fig. 1) are placed before each of the large area photodiodes to prevent from spurious aperturing effects.

We used nematic liquid crystal 5CB dispersed in pure heavy water (D_2O) that leads to the formation of bipolar droplets due to a preferred alignment of the NLC director parallel to the LC/water interface. The D_2O was used to avoid significant temperature rise due to high laser power irradiation, which is approximately 10 times smaller than in the H_2O for the used wavelength. The incident beam polarization is fixed as circular and a trapped bipolar droplet is expectedly put into rotation around the light propagation axis [6,14]. In practice one expects $|s_3^{\text{incident}}| = 1$ for perfectly circular polarization but a residual ellipticity is always observed in practice. Typically we obtain $|s_3^{\text{incident}}| > 0.95$. Note that, in what follows, when looking at s_3 values at the droplet output, the sign of s_3^{incident} is set as negative.

As an example, typical dynamics of Stokes parameters during droplet rotation, $s_1(t)$ (solid line) and $s_3(t)$ (dashed line), are shown in Figure 2 for a $d = 3.4\,\mu\text{m}$ droplet diameter and 400 mW trapping power. Introducing the notation $s_i = \langle s_i \rangle + \text{std}(s_i)$, where $\langle \cdot \rangle$ and $\text{std}(\cdot)$ respectively denote mean value and standard deviation, we obtain $s_1 = 0.028 \pm 0.660$ and $s_3 = -0.211 \pm 0.121$. A regular rigid-body rotation is expected to be characterized by $\langle s_1 \rangle = 0$, $\text{std}(s_1) \neq 0$, $\langle s_3 \rangle = \text{constant}$, and $\text{std}(s_3) = 0$. In the present example, we observe an almost zero mean value of s_1 but the time dependence of s_3 shows oscillations. Such dynamics either indicates a time-varying birefringence Δn_{eff} or is the signature of a residual apparatus anisotropy

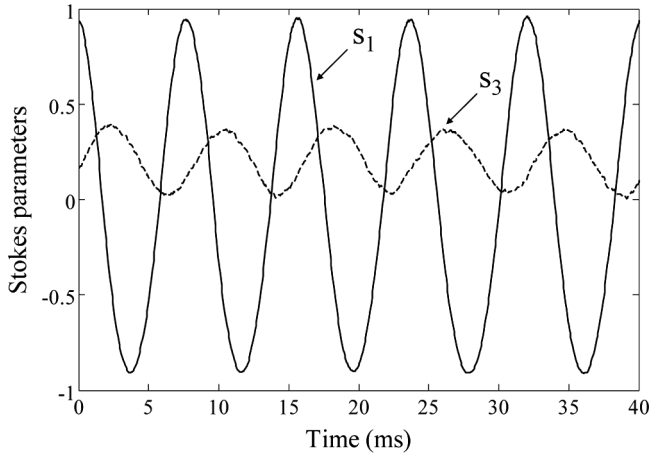

FIGURE 2 Time evolution of the Stokes parameter s_1 (solid line) and s_3 (dashed line) for a 5CB bipolar droplet with diameter $d = 3.4\,\mu m$ for circularly polarized tweezers. Trapping power is 400 mW.

due to non-ideal optical elements. Nevertheless, assuming an ideal situation with perfect polarization conditions, we can estimate the corresponding effective birefringence changes from $s_3 = -\cos\phi$ where $\phi = 2\pi\Delta n_{\text{eff}} d/\lambda$. This gives $\Delta n_{\text{eff}} = 0.089 \pm 0.006$. Obviously, at least a fraction of the few percent of the observed effective birefringence oscillations could be attributed to experimental imperfections. Therefore the unambiguous evidence of an optical reordering that leads to nonlinear rotational motion requires the study of trapping power and droplet diameter dependencies, which is the aim of the next section.

III. NONLINEAR ROTATIONAL REGIMES

In this section, the rotational behavior of bipolar droplets is investigated as a function of trapping power for different droplet diameters. For this purpose, the orientation of the half waveplate used to control the incident power is computer-controlled in order to have a linearly increasing power from one measurement to another, as shown in Figure 3(a). First, we checked that the polarization dynamics apparatus is independent of the input power. Consequently, although there is residual imperfections, as previously mentioned, any departure from a linear behavior of the rotation dynamics with power can safely be attributed to interaction between light and LC orientation changes. Hereafter, the dynamics of the Stokes parameters are measured for

Downloaded by [University of California, San Diego] at 14:19 08 August 2012

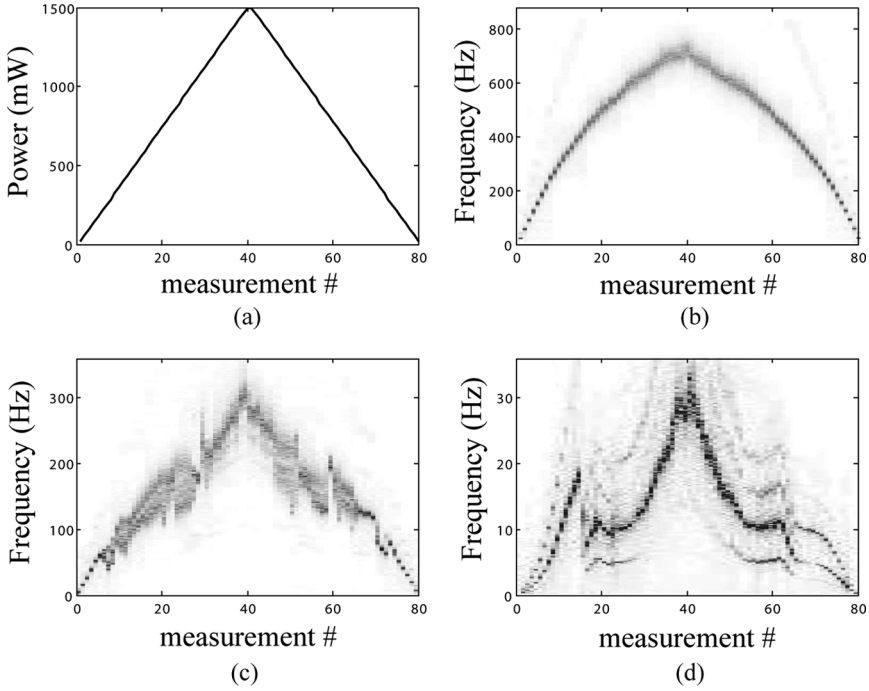

FIGURE 3 (a) Optical trapping power as a function of the measurement number; (b,c,d) Fourier spectra of the s_1 Stokes parameter as a function of measurement number for a droplet diameter $d = 1.4$ (b), 2.7 (c) and 7.2 μm (d), respectively.

40 successive steps with increasing power, up to 1.5 W, followed by 40 additional steps with decreasing power as illustrated in Figure 3(a).

Three different droplet having diameters $d = 1.4$, 2.7 and 7.2 μm have been investigated and Figures 3(b,c,d) show the Fourier spectra of $s_1(t)$ for each case. For a solid birefringent micro-plate one expects single-valued spectra having a linear behavior with respect to trapping power, whose slope depends on the medium thickness. Clearly, this is not the case whatever is the droplet diameter. For the smaller diameter [see Fig. 3(b)] the spectrum is almost single-valued for all powers but the droplet rotation frequency (which is half the peak frequency of s_1 spectrum) exhibits slight deviation from a linear behavior. This is associated with a less effective overall spin angular momentum conversion when the light beam power is increased. Within a solid birefringent plate behavior picture [14], this would be related to a decrease of the effective droplet birefringence. For larger droplet

Downloaded by [University of California, San Diego] at 14:19 08 August 2012

diameters the s_1 spectrum is no longer single-valued and shows a nonlinear behavior with power [see Figs. 3(c,d)] that is characteristic of a complex optical dynamical internal reordering.

Complementary analysis is done by looking at the power dependence of the mean Stokes parameters $\langle s_1 \rangle$ and $\langle s_3 \rangle$. The results are shown in Figure 4 for the same set of droplet diameters as in Figure 3. In Figure 4, increasing and decreasing power are respectively indicated by squares and circles symbols. For a solid birefringent plate behavior one expects $\langle s_1 \rangle = 0$ and $\langle s_3 \rangle =$ constant. On the one hand, the first condition indicates a regular rotational motion or, more generally, a rotational motion that explores positive and negative orientation of the effective optical axis of the droplet in the (x, y) plane over many rotation cycles in a similar manner. On the

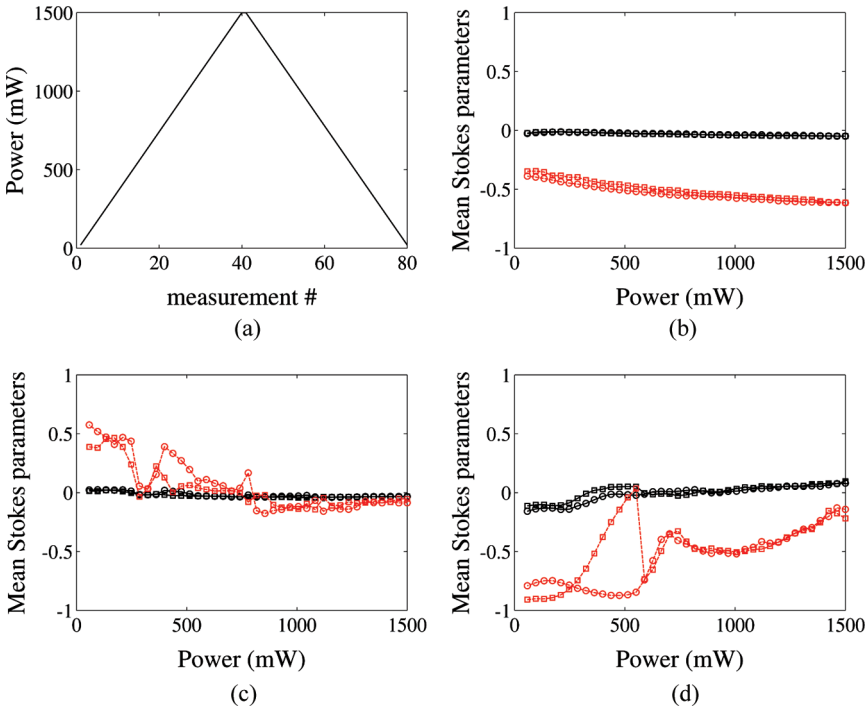

FIGURE 4 (a) Optical trapping power as a function of the measurement number; (b,c,d) Mean values of the Stokes parameters s_1 (black solid line) and s_3 (red dashed line) as a function of power for droplet diameters $d = 1.4$ (b), 2.7 (c) and 7.2 μm (d), respectively. Increasing and decreasing powers are indicated by squares and circles symbols, respectively.

Downloaded by [University of California, San Diego] at 14:19 08 August 2012

other hand, the second condition suggests a non-distorted droplet, namely a constant effective birefringence. From Figure 4(b) we therefore conclude to a regular rotation regime for small droplet diameter, $d = 1.4\,\mu\text{m}$, but with an effective birefringence that smoothly decreases with power. For intermediate droplet diameter, $d = 2.7\,\mu\text{m}$, the rotational motion is slightly perturbed as shown by the irregular behavior of $\langle s_3 \rangle$ with respect to trapping power in Figure 4(c), which is reminiscent of the non single-valued s_1 Fourier spectrum [see Fig. 3(c)]. However we still observe $\langle s_1 \rangle \approx 0$ [see Fig. 4(c)]. For the largest droplet diameter, $d = 7.2\,\mu\text{m}$, the situation is qualitatively different since $\langle s_1 \rangle \neq 0$ and $\langle s_3 \rangle$ strongly varies with power and exhibits a hysteretic behavior [see Fig. 4(d)]. In that case, it is clear that complex dynamical optical reordering takes place and affects the spin angular momentum transfer from light to the LC droplet. Qualitatively, the occurrence of nonlinear dynamics for large droplet diameters can be understood by noting that the larger is the droplet diameter, the smaller is the elastic restoring torque, which scales as $\propto 1/d^2$, and more important is the ability of the optical field to induce significant distorsions. However, a quantitative description of three dimensional light-induced elastic deformations and subsequent angular momentum changes is lacking. Hopefully, recent theoretical developments on finite beam size nonlinear reorientation processes in LCs films in presence of light angular momentum exchanges [17] will help towards a better understanding of this non trivial problem.

Before to conclude, we note that the ratio δ between the beam diameter and the droplet diameter, here $\delta \sim \lambda/d$, is $\delta = 0.7$, 0.4 and 0.15 for $d = 1.4$, 2.7 and $7.2\,\mu\text{m}$, respectively. In fact, it is known that finite beam size effects can lead to complex rotational director dynamics when a NLC film is illuminated by circularly polarized beam having a diameter a few times smaller than the film thickness [20–22]. Interestingly, chaotic rotations were reported in the range $\delta \sim 0.2 - 0.4$ [20–22]. Although these two different kind of systems (droplet vs. film) cannot be compared abruptly, we notice the following general trends: finite beam size effects are related with the occurrence of complex light-induced reorientation dynamics when optical orientational nonlinearities are active.

IV. CONCLUSION

We experimentally studied the rotational regimes of bipolar 5CB nematic liquid crystal droplets in circularly polarized laser tweezers. For this purpose we implemented a dynamical polarization analysis of the trapping beam after it has passed through the droplet and we

Downloaded by [University of California, San Diego] at 14:19 08 August 2012

demonstrated nonlinear rotational dynamics as a function of the trapping beam power. The observed nonlinear behavior is more pronounced for large droplet diameters and emphasizes finite beam size effects to play an important role in the droplet optical reorientation.

REFERENCES

[1] Ashkin, A. (1970). *Phys. Rev. Lett.*, *24*, 156–159.
[2] Misawa, H. & Juodkazis, S. (1999). *Prog. Polym. Sci.*, *24*, 665–697.
[3] Molloy, J. E. & Padgett, M. J. (2002). *Contemp. Phys.*, *43*, 241–258.
[4] Grier, D. G. (2003). *Nature*, *424*, 810–816.
[5] McGloin, D. (2006). *Phil. Trans. R. Soc. A*, *364*, 3521–3537.
[6] Juodkazis, S., Matuso, S., Murazawa, N., Hasegawa, I., & Misawa, H. (2003). *Appl. Phys. Lett.*, *82*, 4657–4659.
[7] Murazawa, N., Juodkazis, S., & Misawa, H. (2006). *Eur. Phys. J. E*, *20*, 435–439.
[8] Gleeson, H. F., Wood, T. A., & Dickinson, M. (2006). *Phil. Trans. R. Soc. A*, *364*, 2789–2805.
[9] Hotta, J.-I., Sasaki, K., & Masuhara, H. (1997). *Appl. Phys. Lett.*, *15*, 2085–2087.
[10] Pattanaporkratana, A., Park, C. S., Maclennan, J. E., & Clark, N. A. (2004). *Ferroelectrics*, *310*, 131–135.
[11] Smalyukh, I. I., Senyuk, B. I., Shiyanovskii, S. V., Lavrentovich, O. D., Kuzmin, A. N., Kachynski, A. V., & Prasad, P. N. (2006). *Mol. Cryst. Liq. Cryst.*, *450*, 79–95.
[12] Smalyukh, I. I., Kaputa, D. S., Kachynski, A. V., Kuzmin, A. N., & Prasad, P. N. (2007). *Opt. Express*, *15*, 4359–4371.
[13] Friese, M. E. J., Nieminen, T. A., Heckenberg, N. R., & Rubinsztein-Dunlop, H. (1998). *Nature (London)*, *394*, 348–350.
[14] Wood, T. A., Gleeson, H. F., Dickinson, M. R., & Wright, A. J. (2004). *Appl. Phys. Lett.*, *84*, 4292.
[15] Tabiryan, N. V., Sukhov, A. V., & Zel'dovich, B. Ya. (1986). *Mol. Cryst. Liq. Cryst.*, *136*, 1.
[16] Murazawa, N., Juodkazis, S., & Misawa, H. (2006). *Opt. Express*, *14*, 2481.
[17] Brasselet, E., Murazawa, N., Juodkazis, S., & Misawa, H. (2008). *Phys. Rev. E*, *77*, 041704.
[18] Yang, Y., Brimicombe, P. D., Roberts, N. W., Dickinson, M. R., Osipov, M., & Gleeson, H. F. (2008). *Opt. Express*, *16*, 6877.
[19] Manzo, C., Paparo, D., Marrucci, L., & Jánossy, I. (2006). *Phys. Rev. E*, *73*, 051707.
[20] Vella, A., Setaro, A., Piccirillo, B., & Santamato, E. (2003). *Phys. Rev. E*, *67*, 051704.
[21] Brasselet, E. & Dubé, L. J. (2006). *Phys. Rev. E*, *73*, 021704.
[22] Brasselet, E., Piccirillo, B., & Santamato, E. (2008). *Phys. Rev. E*, *78*, 031703.

Downloaded by [University of California, San Diego] at 14:19 08 August 2012